Author(s): Ivanov, Daniil M.; Kinzhalov, Mikhail A.; Novikov, Alexander S.; Ananyev, Ivan V.; Romanova, Anna A.; Boyarskiy, Vadim P.; Haukka, Matti; Kukushkin, Vadim Yu.

Title: The H2C(X)–X•••X– (X = Cl, Br) Halogen Bonding of Dihalomethanes

Year: 2017

Version:

Please cite the original version:

Ivanov, D. M., Kinzhalov, M. A., Novikov, A. S., Ananyev, I. V., Romanova, A. A., Boyarskiy, V. P., Haukka, M., & Kukushkin, V. Y. (2017). The H2C(X)–X•••X– (X = Cl, Br) Halogen Bonding of Dihalomethanes. Crystal Growth and Design, 17(3), 1353-1362. https://doi.org/10.1021/acs.cgd.6b01754

Article

The HC(X)–X•••X (X = Cl, Br) Halogen Bonding of Dihalomethanes

Daniil M. Ivanov, Mikhail A. Kinzhalov, Alexander S. Novikov, Ivan V Ananyev, Anna A. Romanova, Vadim P. Boyarskiy, Matti Haukka, and Vadim Yu. Kukushkin

Cryst. Growth Des., **Just Accepted Manuscript** • DOI: 10.1021/acs.cgd.6b01754 • Publication Date (Web): 18 Jan 2017

The $H_2C(X)–X•••X^-$ (X = Cl, Br) Halogen Bonding of Dihalomethanes

Daniil M. Ivanov,† Mikhail A. Kinzhalov,† Alexander S. Novikov,† Ivan V. Ananyev,◊ Anna A. Romanova,◊ Vadim P. Boyarskiy,† Matti Haukka,§ and Vadim Yu. Kukushkin,†*

† Saint Petersburg State University, Universitetskaya Nab. 7/9, 199034 Saint Petersburg, Russian Federation

◊A. N. Nesmeyanov Institute of Organoelement Compounds, Russian Academy of Sciences, 119991, Vavilova St., 28, Moscow, Russian Federation

§ Department of Chemistry, University of Jyväskylä, P.O. Box 35, FI-40014 Jyväskylä, Finland

Abstract

The dihalomethane–halide $H_2C(X)–X•••X^-$ (X = Cl, Br) halogen bonding was detected in a series of the *cis*-[PdX(CNCy){C(NHCy)=NHC$_6$H$_2$Me$_2$NH$_2$}]X•CH_2X_2 (X = Cl, Br) associates by single-crystal XRD followed by DFT calculations. Although ESP calculations demonstrated that the σ-hole of dichloromethane is the smallest among all halomethane solvents (the maximum electrostatic potential is only 2.6 kcal/mol), the theoretical DFT calculations followed

by Bader's QTAIM analysis (M06/DZP-DKH level of theory) confirmed the $H_2C(X)–X•••X^-$ halogen bond both in the solid state and gas phase optimized geometries. The estimated bonding energies in $H_2C(X)–X•••X^-$ is in the 1.9–2.8 kcal/mol range.

Introduction

Orientation of solvent molecules around anions is intensively studied in crystal engineering, solution and colloid chemistry, and also in catalysis.[1-7] Among different anions, halides play especially important chemical and biological roles, in particular, in asymmetric catalysis,[8-10] design of artificial anion receptors, and in the ionic homeostasis of the living cells.[11-15] In most cases, solvation of halide anions proceeds through hydrogen bonding (HB) with solvent molecules.

Halomethanes—apart from positive H centers responsible for HBs—featuring an alternative type of partial positive charge centers, viz. the σ-holes[16] of covalently bound chlorine, bromine, or iodine atoms, which may be responsible for non-covalent contacts. The calculations conducted by us in this work (**Table 1**, **Figure 1**) and previously by some other groups[17-19] (for more details see Supporting information, **Table SI1**) clearly indicate that the values of electrostatic potential on the σ-holes, and correspondingly the ability of forming XBs, substantially depend on amount and type of halogen atoms in the halomethanes. These XBs were widely studied for *effective* halomethane XB donors (CBr_4,[19-21] CHI_3,[22,23] $CFBr_3$,[19] CCl_3Br,[24] and $CHBr_3$;[19,20] for full description of the $C–X•••X^-$ XBs, the $X•••X^-$ distances and the $\angle(C–X•••X^-)$ angles see Supporting information, **Table SI2**), whereas the relatively *inactive* (**Table 1**, **Figure 1**) XB donors such as CCl_4 and $CHCl_3$ quite rarely form XBs.[25-26]

Table 1. Maximum electrostatic potentials ($V_S(\mathbf{r})_{max}$, kcal/mol) on the halogen atoms calculated (see Experimental) on the 0.001 a.u. molecular surfaces for CH_3X, CH_2X_2, CHX_3, and CX_4 (X = Cl, Br, I) structures optimized (the M06-2X/CEP-121G level of theory) in gaseous phase ("values" of σ-holes). The "values" of σ-holes as a percentage of the maximal are given in parentheses.

X	Cl	Br	I
CH_3X	–7.7	4.8 (15%)	15.1 (48%)
CH_2X_2	2.6 (8%)	13.7 (43%)	23.1 (73%)
CHX_3	10.4 (33%)	19.9 (63%)	28.1 (89%)
CX_4	16.0 (51%)	24.1 (77%)	31.5 (100%)

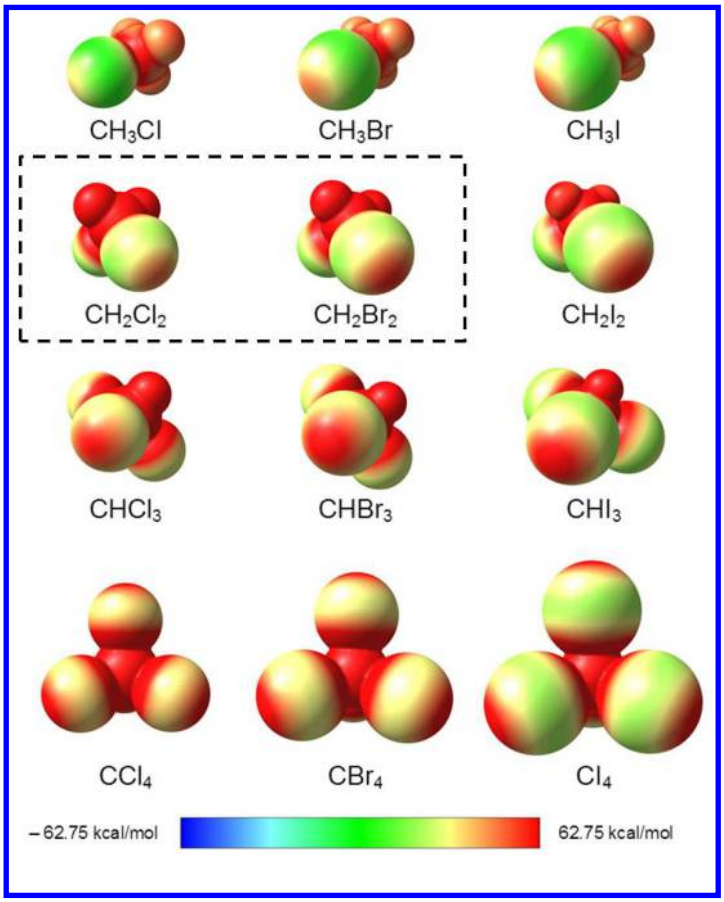

Figure 1. ESP distribution in the CH_nX_{4-n} (X = Cl, Br, I; n = 1–3) halomethane molecules.

Until now only a few publications were devoted to XBs in condensed phases involving CH_2Cl_2, as the weakest σ-hole donor among halomethane solvents, and also with its bromine congener, CH_2Br_2. Thus, the possibility of CH_2Cl_2 to behave as XB donor was acknowledged by statistical analyses of CCDC structures conducted by Allen *et al*.[27] and Mooibroek *et al*.[28] In the former report,[27] a possibility for the formation of various $H_2C(Cl)–Cl•••X–C$ (X = Cl, Br, I) short contacts was indicated, but the angle parameters were not specified and therefore the ability of CH_2Cl_2 behave as XB donor was not fully confirmed. The latter article[28] gives certain statistical evidences favoring $H_2C(Cl)–Cl•••D$ (D = F, Cl, Br, I, N, O, S) contacts, which can be treated as dichloromethane-involved XBs.

Rodríguez and Bertrán[29] conducted NMR correlation analysis for CH_2X_2 (X = Cl, Br, I) in solvents of different basicity. The observed differences in ^1H chemical shifts indicated that behavior of CH_2Cl_2 and CH_2Br_2 in these solutions is almost the same and the contribution of XBs to the solvation process is expected to be identical. Insofar as it was assumed[29] that CH_2Cl_2 forms only HB, it collaterally means that CH_2Br_2 does not form XBs in solutions. Jin *et al.*[17] recently carried out EPR correlation study of the solvation of 2,2,6,6-tetramethyl-1-piperidin-1-yloxy free radical (TEMPO) by various solvents—including CH_2Cl_2 and CH_2Br_2—and found that the solvation is different in halogenated and in halogen-free solvents because of the C–X•••˙O–N XB. Subsequent theoretical calculations demonstrated comparable energies of HB and XB in the observed solvent–TEMPO weak interactions.

In the solid state, dibromomethane forms the $H_2C(Br)–Br•••Br–C$,[30,31] $H_2C(Br)–Br•••O$,[32] and $H_2C(Br)–Br•••N$[33] types of XB. Concurrently, XBs involving CH_2Cl_2 as the weakest XB donor among halomethane solvents, were described only in three works. The $H_2C(Cl)–Cl•••Cl–C$ XBs were found in the crystalline CH_2Cl_2[34] and the unusual $H_2C(Cl)–Cl•••N≡[Os]$ halogen bonds were discussed in a review.[35] Eventually, some of us recently reported that CH_2X_2 (X = Cl, Br) form the $H_2C(X)–X•••Cl–[Pt]$ (X = Cl, Br) XBs with chloride ligands in platinum(II) PANT complexes.[36] In the context of this work, one should stress that XBs of CH_2Cl_2 or CH_2Br_2 with *any of the halide anions* are yet unreported.

Previously we demonstrated that cationic 1,3,5-triazapentadienato nickel(II) and platinum(II) complexes can be used as scaffolds for a numerous solvent–chloride clusters held by simultaneous HBs [26,37-40] and XBs.[26] We now expand a range of metal-based platforms, which can be applied for recognition of novel types of XB, by using acyclic diaminocarbene

palladium(II) complexes (**Scheme 1**) known as catalysts for various organic transformations.[41-47] We found that these palladium species can be co-crystallized with very weak XB donors such as dichloromethane and dibromomethane giving solvates featuring $H_2C(X)–X•••X^-$ (X = Cl, Br) XBs and our findings are the first recognition of XB between uncomplexed halides and dihalomethanes.

Results and Discussion

Recently we reported[48,49] the reaction between *cis*-$[PdCl_2(CNR^1)_2]$ (**1**) and benzene-1,2-diamines (**2**) that leads to the *cis*-$[PdCl(CNR^1)\{\underline{C}(NHR^1)=NHC_6H_2(R^2)_2\underline{N}H_2\}]Cl$ (R^1 = Cy (cyclohexyl), 2-Cl-6-MeC_6H_3, 2,6-$Me_2C_6H_3$; R^2 = H, Me, Cl, **3a**–**d**) complexes bearing Cl^- as the counterion (**Scheme 1**). Complexes **3b**, **3c**, and **3d** (**Table 1**) were characterized by single-crystal X-ray diffraction (XRD) as dichloromethane solvates **3b**•CH_2Cl_2, **3c**•1½CH_2Cl_2, and **3d**•CH_2Cl_2•H_2O (**Figure 2**, left).[48,50] In these three structures, only N–H•••Cl^-, O–H•••Cl^- (in **3d**•CH_2Cl_2•H_2O), and C–H•••Cl^- hydrogen bonds were observed and no halogen bonds were detected.

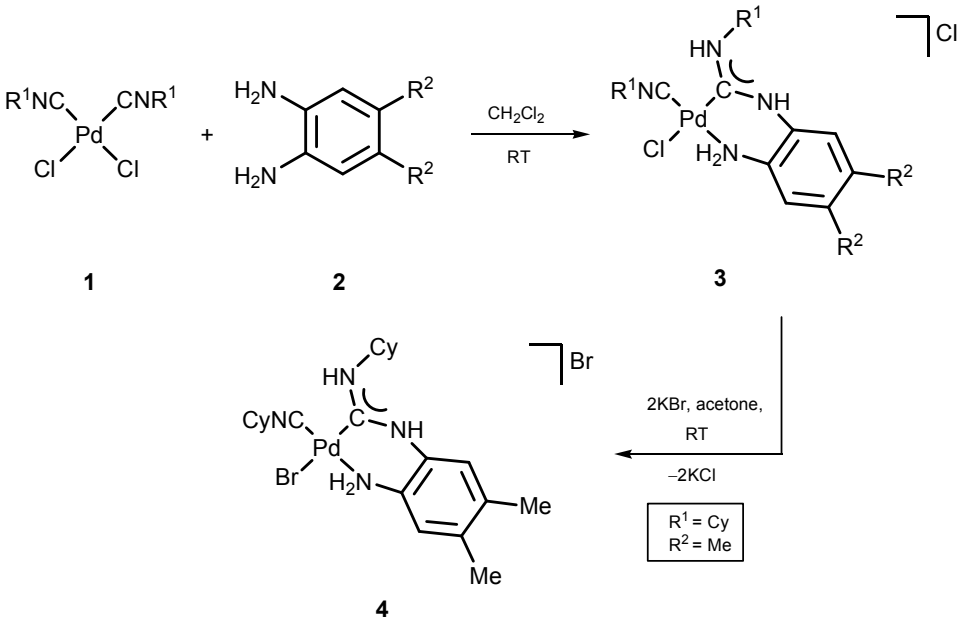

Scheme 1. Syntheses of **3** and **4**.

Table 2. Numbering of complexes and their halomethane associates.

Complex	**R^1**	**R^2**	**CH_2X_2**	**Associate**	**X-ray**
3a	Cy	Me	CH_2Cl_2	**3a**•CH_2Cl_2	This work
3a	Cy	Me	CH_2Br_2	**3a**•CH_2Br_2	This work
3b	2-Cl-6-MeC_6H_3	Me	CH_2Cl_2	**3b**•CH_2Cl_2	Ref[48]
3c	2-Cl-6-MeC_6H_3	Cl	CH_2Cl_2	**3c**•1½CH_2Cl_2	Ref[48]
3d	2,6-$Me_2C_6H_3$	Me	CH_2Cl_2	**3d**•CH_2Cl_2•H_2O	Ref[50]
4	Cy	Me	CH_2Cl_2	**4**•CH_2Cl_2	This work
4	Cy	Me	CH_2Br_2	**4**•CH_2Br_2	This work

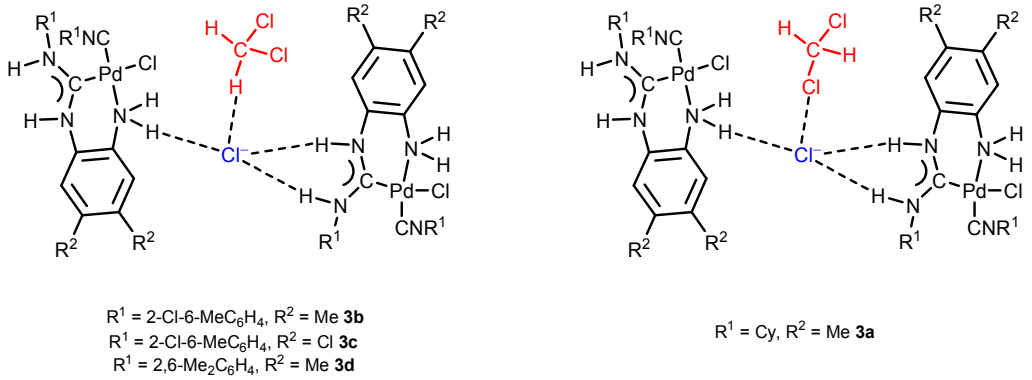

Figure 2. The environment of Cl^- in previously reported solvates **3b**•CH_2Cl_2, **3c**•1½CH_2Cl_2, and **3d**•CH_2Cl_2•H_2O (left) and in **3a**•CH_2Cl_2 studied in this work (right).

We now found that **3a** is crystallized with dichloromethane giving **3a**•CH_2Cl_2, where the $H_2C(Cl)$–Cl•••Cl^- short contacts (**Figure 2**, right) were identified. These contacts can be interpreted as XBs accordingly to the IUPAC "distance" and "angle" criteria.[51] Indeed, the distances d(Cl•••Cl) = 3.276(3) and 3.236(3) Å are sufficiently less than the sum of the Rowland's vdW[52] radii ($2R_{vdW}$(Cl) = 3.52 Å) and the angles ∠(C–Cl•••Cl) = 166.3(3) and 166.2(4)° are close to 180°. We found that only **3a**, among all other species derived from the coupling with benzene-1,2-diamine, gives dichloromethane solvate with XB. We believe that this is due to the crucial role of the shape of the molecular cation of **3a** in the crystal packing and, consequently, in the formation of XB. The replacement of cyclohexyl substituents to aryls in the starting complex and methyl substituents to chlorine atoms in the starting nucleophile lead to another environment of the chloride anion (**Figure 2**, left) and even to another complex:dichloromethane ratio in **3c**•1½CH_2Cl_2 and to the inclusion of water in **3d**•CH_2Cl_2•H_2O.

We also succeeded to perform the CH_2Cl_2/CH_2Br_2 isostructural exchange[53,54] with complete preservation of the solvent environment in **3a**•CH_2Br_2.[32,36,55] In the X-ray structure of **3a**•CH_2Br_2, the $H_2C(Br)–Br•••Cl^-$ XBs were found (d(Br•••Cl) = 3.1911(11) Å is less than Rowland's $R_{vdW}(Cl) + R_{vdW}(Br)$ = 3.63 Å, and ∠(C–Br•••Cl) is 167.3(2)°). Despite significant difference in the cell parameters of **3a**•CH_2Cl_2 and **3a**•CH_2Br_2, these two species demonstrate similar crystal structures, and positions of each complex cation, chloride anion, and solvent molecule are almost the same (**Figure 3**, **a**–**b**).

To expand a number of dihalomethane–halide clusters, complex **4** was obtained by the metathetical reaction of **3a** with KBr (**Scheme 1**), whereupon **4** was co-crystallized with CH_2Cl_2 and CH_2Br_2 forming solvates **4**•CH_2Cl_2 and **4**•CH_2Br_2, respectively. In the structure of **4**•CH_2Cl_2, the positions of the complex cations and bromide counterions are close to those found for **3a**•CH_2Cl_2, but solvent molecules are arranged differently and the $Cl_2C(H)–H•••Br^-$ HBs were found instead XBs (**Figure 3**, **c**). This observation can be accounted for by the lower XB energy in the case of CH_2Cl_2 than that in CH_2Br_2 (see theoretical considerations for details later). The difference between **3a**•CH_2Cl_2 and **4**•CH_2Cl_2 in terms of their ability of forming XBs *vs.* HBs, were also indirectly observed by IR spectroscopy in the solid state (see SI, **Figure SIV4**), when we found a change of shapes of the antisymmetric C–Cl stretches. The high temperature (300 K) XRD experiment for **4**•CH_2Cl_2 indicated that CH_2Cl_2 is fully disordered, occupying at least three different positions and therefore reliable information on solvent-involved weak interactions could not be obtained.

In the case of **4**•CH_2Br_2, the released single-crystals are unstable at 100 K probably due to a phase transition and data collection was performed at 200 K. The structure of **4**•CH_2Br_2 is close to **3a**•CH_2Br_2 (**Figure 3**, **d** and **Figure 4**, **d**), and the $H_2C(Br)–Br•••Br^-$ short contacts

referred to XB insofar as *d*(Br•••Br) = 3.3137(8) Å is less than Rowland's $2R_{vdW}$(Br) = 3.74 Å, and ∠(C–Br•••Br) is 169.4(2)°. These values agree well with both geometrical IUPAC criteria[51] for XB.

In **3a**•CH_2Cl_2, **3a**•CH_2Br_2, **4**•CH_2Cl_2, and **4**•CH_2Br_2, apart from XBs numerous N–H•••X^-, C–H•••X^-, N–H•••X–Pd, and C–H•••X–Pd (X = Cl, Br) HB's were identified (see Supporting information).

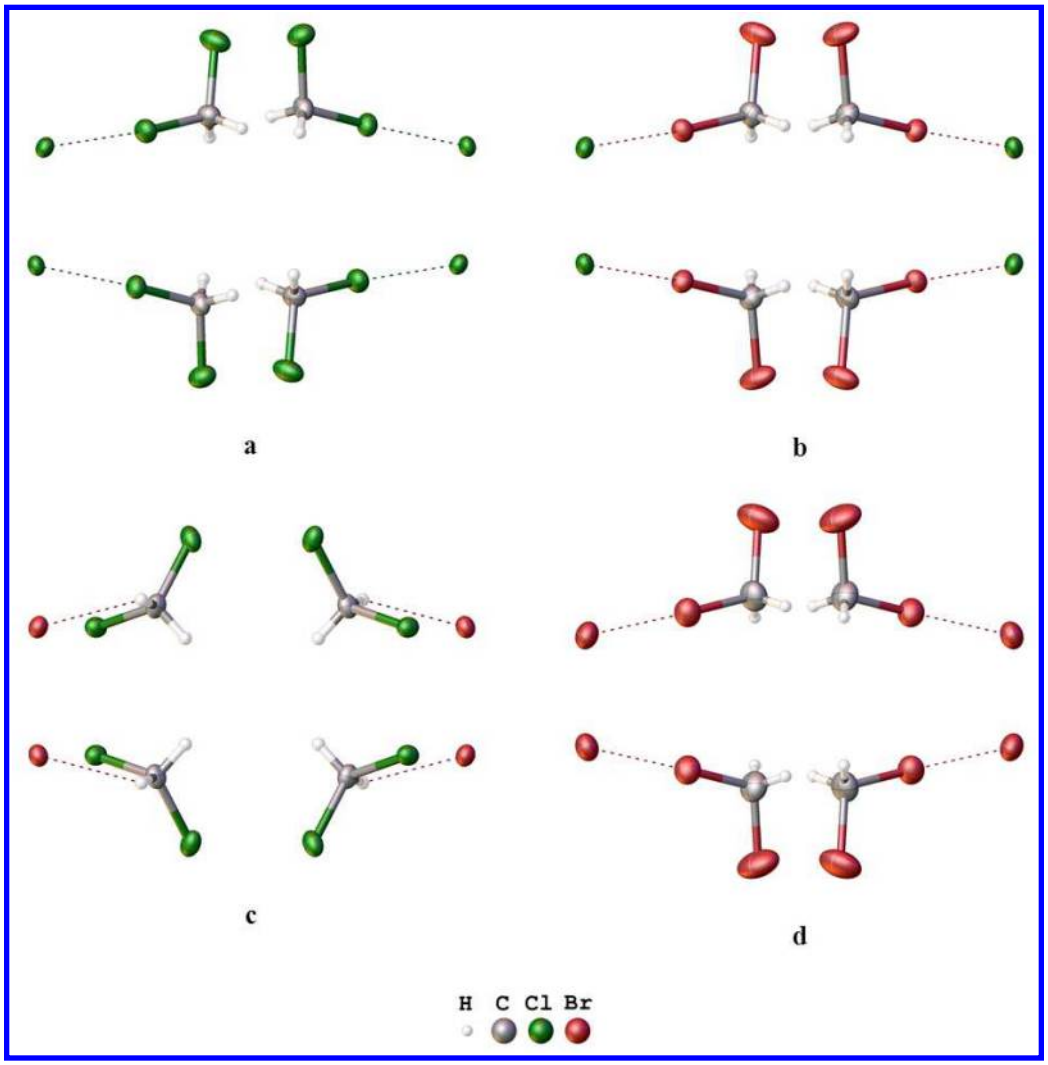

Figure 3. Packing of dihalomethane molecules and halide anions in **3a**•CH_2Cl_2 (**a**), **3a**•CH_2Br_2 (**b**), **4**•CH_2Cl_2 (**c**), and **4**•CH_2Br_2 (**d**). Thermal ellipsoids are given at the 50% probability level.

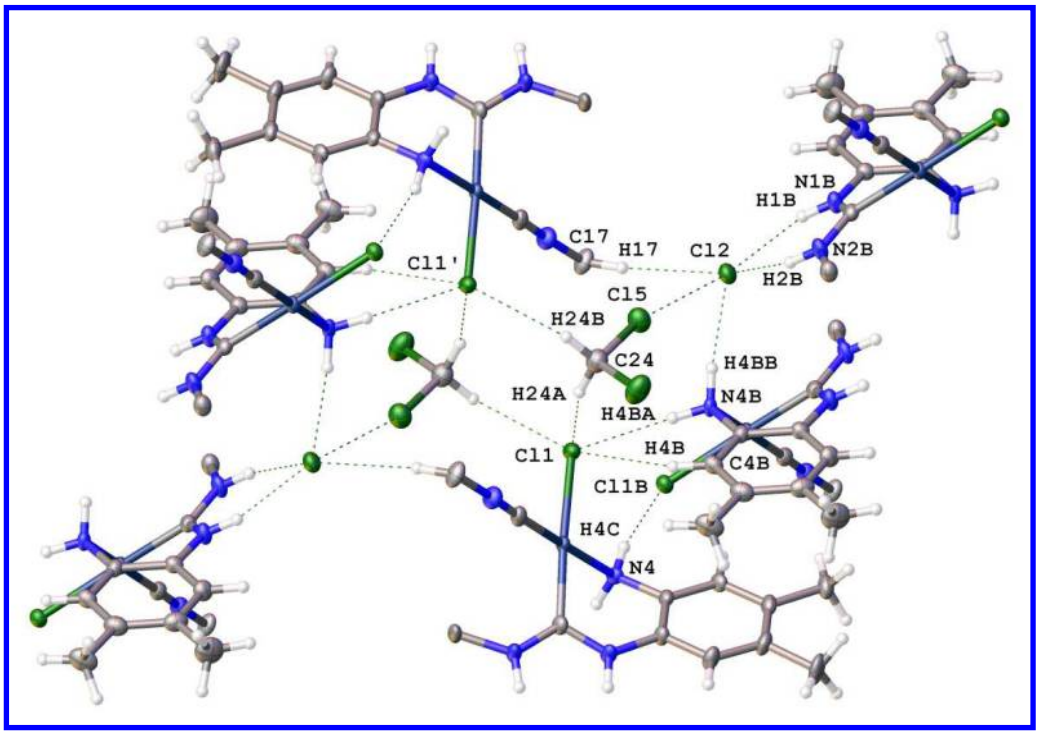
N1B
H1B
C17
H17
C12
N2B
Cl1'
H2B
C15
H24B
C24
H4BB
H24A
N4B
H4BA
H4B
Cl1
C4B
Cl1B
H4C
N4

a1

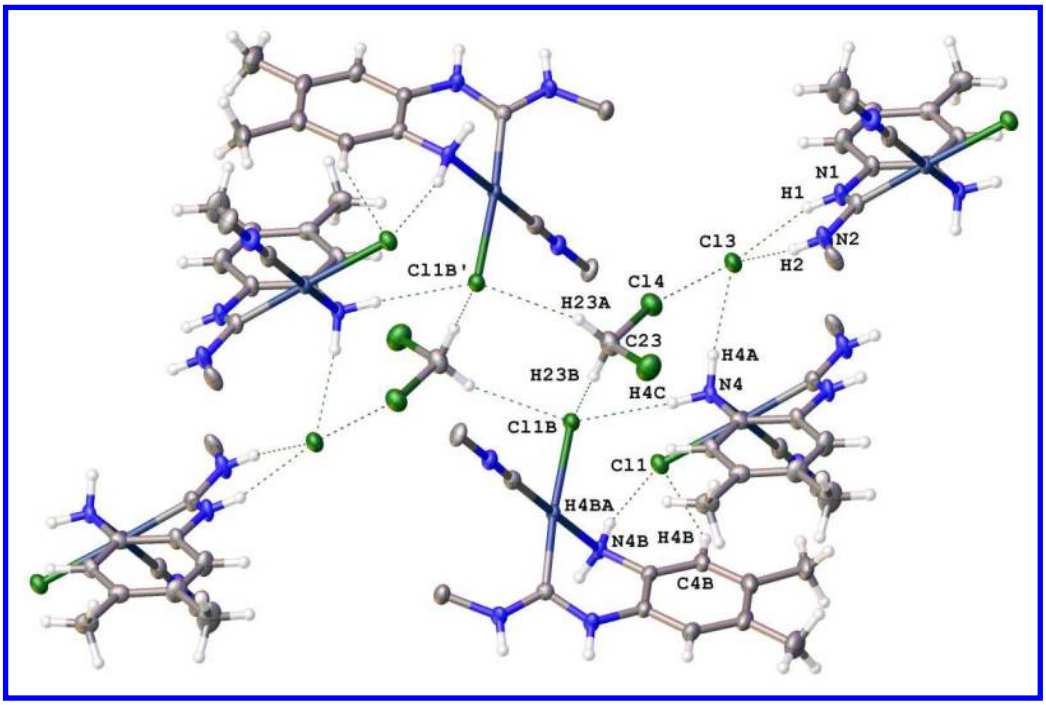
N1
H1
C13
N2
H2
Cl1B'
C14
H23A
C23
H4A
H23B
H4C
N4
Cl1B
Cl1
H4BA
N4B
H4B
C4B

a2

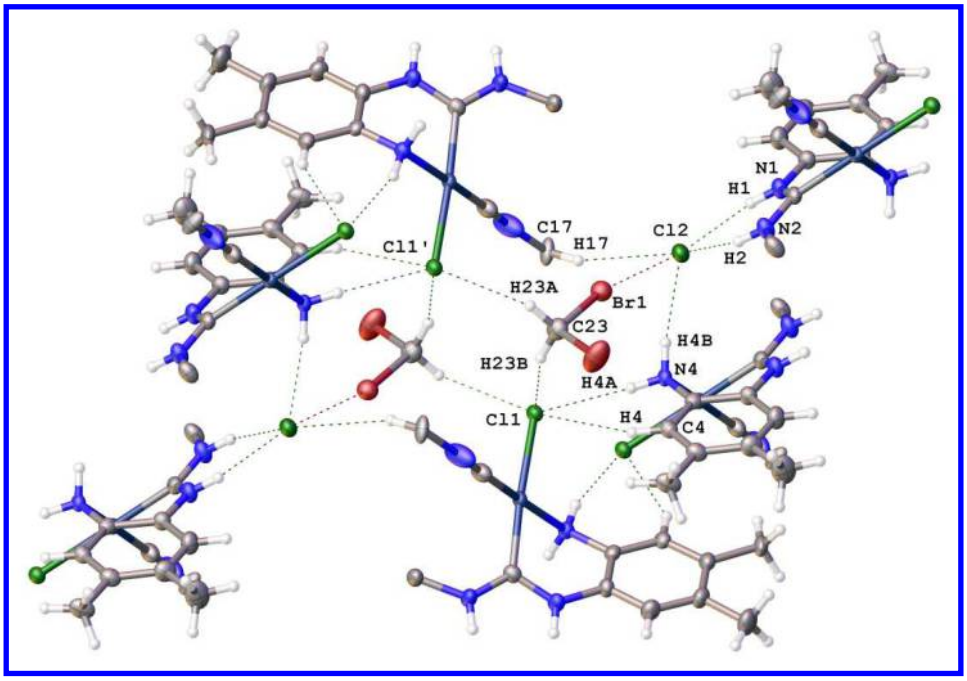
N1
H1
C17
H17
C12
N2
H2
Cl1'
H23A
Br1
C23
H4B
H23B
N4
H4A
Cl1
H4
C4

b

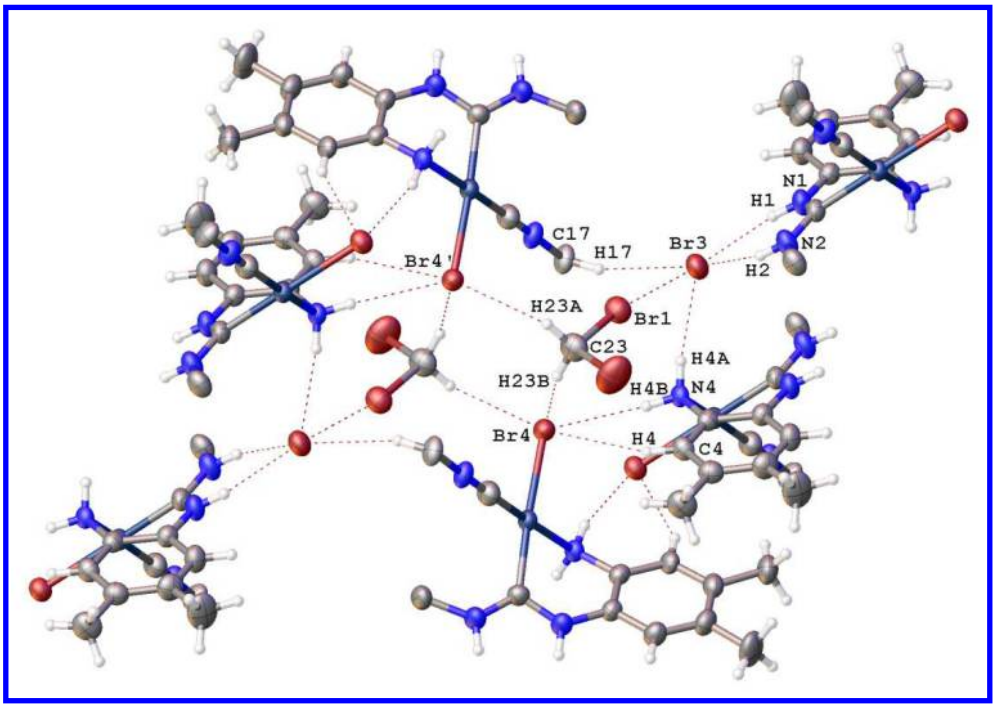
N1
H1
C17
H17
Br3
N2
Br4
H2
H23A
Br1
C23
H4A
H23B
H4B
N4
Br4
H4
C4

c

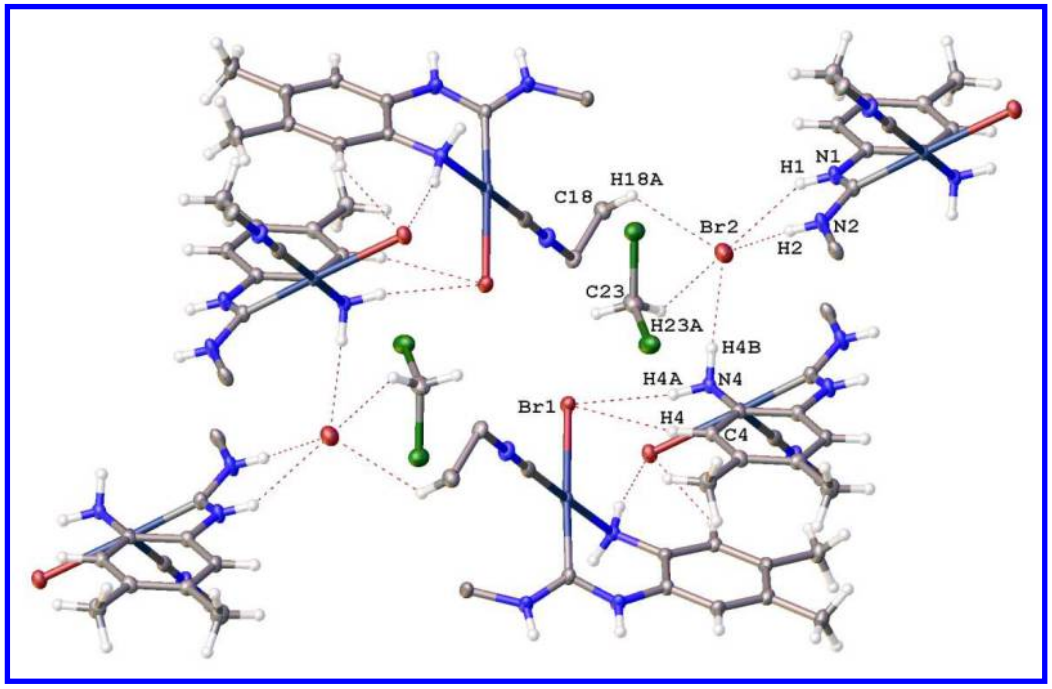
H1
N1
H18A
C18
Br2
N2
H2
C23
H23A
H4B
H4A
N4
Br1
H4
C4

d

Figure 4. Two types of isostructural fragments in **3a**•CH_2Cl_2 (**a1**, **a2**) and analogous fragments in **3a**•CH_2Br_2 (**b**), **4**•CH_2Br_2 (**c**), and **4**•CH_2Cl_2 (**d**). Cyclohexyl rings were omitted for clarity. Thermal ellipsoids are given at the 50% probability level.

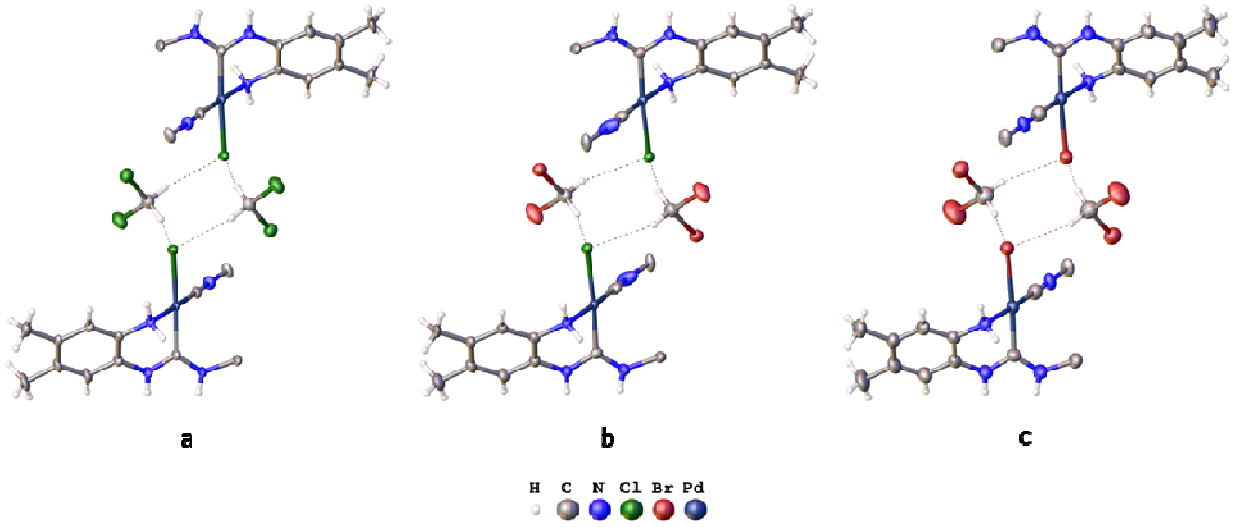

Figure 5. One of the heterotetrameric clusters in **3a**•CH_2Cl_2 (**a**) and the analogous clusters in **3a**•CH_2Br_2 (**b**), and **4**•CH_2Br_2 (**c**). Cyclohexyl rings were omitted for clarity. Thermal ellipsoids are given at the 50% probability level.

Noteworthy that in **3a**•CH_2Cl_2, **3a**•CH_2Br_2, and **4**•CH_2Cl_2, we observed the heterotetrameric clusters (**Figure 5**) that consist of two complex cations and two solvent molecules with two types of the $X_2C(H)$–H•••X–Pd (X = Cl, Br) HB's. Electrostatic repulsion between the negatively charged halide ligands is shielded by two solvent molecules. Similar clusters were previously reported by us,[36] and these species contain two neutral chloride platinum(II) complexes and two dihalomethane molecules, simultaneously linked by two $X_2C(H)$–H•••Cl–Pt HB's and two $H_2C(X)$–X•••Cl–Pt (X = Cl, Br) XB's.

Table 3. The parameters of the $H_2C(X)–X•••Cl^–$ (X = Cl, Br) XBs.

Solvate	C–X•••Cl⁻	*d*(X•••Cl), Å	R_{ClX}	∠(C–X•••Cl),°	E_{int}^{a*}	E_{int}^{b*}
3a•CH_2Cl_2	C24–Cl5•••Cl2⁻	3.276(3)	0.93	166.3(3)	1.9	2.2
	C23–Cl4•••Cl3⁻	3.236(2)	0.92	166.2(4)	2.2	2.2
3a•CH_2Br_2	C23–Br1•••Cl2⁻	3.1911(11)	0.88	167.3(2)	2.8	2.7
4•CH_2Br_2	C23–Br1•••Br3⁻	3.3137(8)	0.89	169.4(2)	2.5	2.4
	Comparison**	3.52 (Cl•••Cl)	1.00	180		
		3.63 (Br•••Cl)				
		3.74 (Br•••Br)				

* *The strength of these weak interactions (in kcal/mol) has been defined according to the procedures proposed by Espinosa et al. ($E_{int}^{a} = –V(\mathbf{r})/2$)[56] and Vener et al. ($E_{int}^{b} = 0.429G(\mathbf{r})$),[57] these approaches considered explore linear relationships between potential energy V(**r**) and Lagrangian kinetic energy G(**r**) densities at the bond critical points and energies of appropriate contacts.*

** *"Comparison" is the sum of Rowland's vdW radii and the classic XB angle.*

Theoretical considerations. Inspection of the crystallographic data for dihalomethane solvates **3a**•CH_2Cl_2, **3a**•CH_2Br_2, and **4**•CH_2Br_2 suggests the availability of Cl•••Cl⁻ and Br•••Cl⁻ XBs and along with the presence different types of HBs. To confirm the existence of these weak XB interactions from theoretical viewpoint and evaluate their energies, we performed DFT calculations followed by Bader's QTAIM analysis.[58] We have successfully used this approach upon studies of non-covalent interactions and properties of coordination bonds in various transition metal complexes.[36,40,59-65] The model systems were isolated from the experimental X-ray data as three large clusters (*cis*-[PdCl(CNCy){C(NHCy)=NHC$_6$H$_2$Me$_2$NH$_2$}]$^+$)$_6$•(Cl$^–$)$_2$•(CH$_2$X$_2$)$_2$ (X = Cl, two types, see

Figure 2, **a**–**b**; X = Br, **c**), which include all types of short contacts. Results of QTAIM analysis are summarized in **Table 4** (XBs) and **Table SV2** (HBs).

Table 4. Values of the density of all electrons – ρ(**r**), Laplacian of electron density – $\nabla^2\rho(\mathbf{r})$, energy density – H_b, potential energy density – V(**r**), and Lagrangian kinetic energy – G(**r**) (Hartree) at the bond critical points (3, –1), corresponding to the $H_2C(X)–X\bullet\bullet\bullet Cl^-$ (X = Cl, Br) XBs.

Solvate	C–X•••X⁻	type**	d(X•••X⁻)	ρ(**r**)	$\nabla^2\rho(\mathbf{r})$	H_b	V(r)	G(r)	E_{int}^{a*}	E_{int}^{b*}
3a•CH_2Cl_2	C24–Cl5•••Cl2⁻	exp.	3.276	0.011	0.037	0.002	–0.006	0.008	1.9	2.2
		free	3.276	0.012	0.035	0.001	–0.006	0.007	1.9	1.9
		opt.	2.963	0.020	0.062	0.002	–0.012	0.014	3.8	3.8
	C23–Cl4•••Cl3⁻	exp.	3.236	0.011	0.040	0.002	–0.007	0.008	2.2	2.2
		free	3.236	0.013	0.037	0.001	–0.007	0.008	2.2	2.2
		opt.	2.966	0.020	0.061	0.002	–0.012	0.014	3.8	3.8
3a•CH_2Br_2	C23–Br1•••Cl2⁻	exp.	3.191	0.014	0.048	0.002	–0.009	0.010	2.8	2.7
		free	3.191	0.016	0.044	0.001	–0.008	0.010	2.5	2.7
		opt.	2.941	0.024	0.071	0.001	–0.015	0.016	4.7	4.3
	***C–Cl•••Br⁻	opt.	3.072	0.021	0.050	0.000	–0.012	0.012	3.8	3.2
4•CH_2Br_2	C23–Br1•••Br3⁻	exp.	3.314	0.014	0.038	0.001	–0.008	0.009	2.5	2.4
		free	3.314	0.016	0.034	0.000	–0.008	0.008	2.5	2.2
		opt.	3.016	0.025	0.060	0.000	–0.015	0.015	4.7	4.0

* *The strength of these weak interactions (in kcal/mol) has been defined according to the procedures proposed by Espinosa et al. ($E_{int}^{a} = -V(\mathbf{r})/2$)[56] and Vener et al. ($E_{int}^{b} = 0.429G(\mathbf{r})$),[57] these approaches considered explore linear relationships between potential energy V(**r**) and Lagrangian kinetic energy G(**r**) densities at the bond critical points and energies of appropriate contacts.*

** *Type of calculations: exp. – single point calculations based on the experimental X-ray geometries for the large clusters $(cis\text{-}[PdX(CNCy)\{\underline{C}(NHCy)=NHC_6H_2Me_2\underline{N}H_2\}]^+)_6\bullet(X^-)_2\bullet(CH_2X_2)_2$, free – single point calculations based on the experimental X-ray geometries for*

the small clusters $(X^-)\bullet(CH_2X_2)$, opt. – single point calculations based on the optimized gas phase geometries for the small clusters $(X^-)\bullet(CH_2X_2)$.
*** *Only the optimized structure for C–Cl•••Br⁻.*

The QTAIM analysis allows the verification of several bond critical points (BCP's) (3, –1) for XBs C–X•••X⁻ (X = Cl, Br) (**Table 4**) and different HB's (**Table SV2**). The low magnitude of the electron density, positive values of the Laplacian, and very close to zero energy density in these BCP's are typical for non-covalent interactions. The relation $-G(\mathbf{r})/V(\mathbf{r}) \geq 1$ for all BCP's listed in **Tables 4** and **SV2**, and points out that the nature of these interactions is purely non-covalent.[66] The small values of the Wiberg bond indices for C–X•••X⁻ contacts in the optimized structures (viz. 0.08–0.18) computed by using the natural bond orbital (NBO) partitioning scheme additionally confirm the electrostatic nature of these non-covalent interactions.

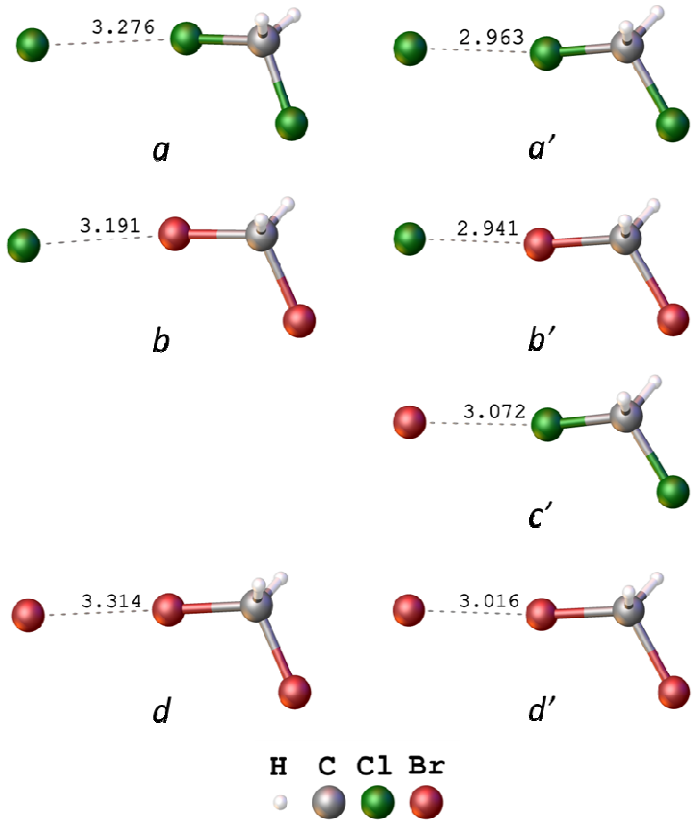

Figure 6. Experimental (left) and optimized (right) structures of the (X–)•(CH_2X_2) clusters, length unit – Å.

We attempted to estimate the effect of short-range environment and crystal packing on the energies of XBs in the studied systems. For these purposes we isolated the small clusters (Cl^-)•(CH_2Cl_2) (**Figure 6**, *a*), (Cl^-)•(CH_2Br_2) (*b*), and (Br^-)•(CH_2Br_2) (*d*) from the experimental X-ray geometries of **3a**•CH_2Cl_2, **3a**•CH_2Br_2, and **4**•CH_2Br_2, respectively, and carried out single point calculations and QTAIM analysis (in this case only short-range environment effect is excluded from the consideration). Then we performed geometry optimization procedure followed by the single point calculations and QTAIM analysis (in that case both effects are not taking into account). For the cluster (Br^-)•(CH_2Cl_2), the starting (Cl^-)•(CH_2Cl_2) geometry followed by the Cl^-/Br^- exchange was used (**Figure 6**, *c*). Our results are presented in **Table 4**

("free" for the starting experimental geometries, "opt." for the optimized geometries). It is clear that short-range environment virtually does not affect the energies of XBs, but the influence of crystal packing is much more significant. Indeed, geometry optimization leads to shortening of the Br•••Cl^-, Cl•••Cl^-, and Br•••Br^- contacts by 0.250–0.313 Å and to their approximately two-fold strengthening. Noteworthy that the optimized structures *a–d* exhibit similar structural motifs. The contour line diagrams of the Laplacian distribution $\nabla^2\rho(\mathbf{r})$, bond paths and selected zero-flux surfaces for the optimized (X^-)•(CH_2X_2) clusters are shown in **Figure 7**. To visualize XBs in the studied systems, reduced density gradient (RDG) analysis[67] was carried out. The RDG isosurfaces reveal the presence of $H_2C(X)–X•••X^-$ (X = Cl, Br) non-covalent interactions in optimized structures of (Cl^-)•(CH_2Cl_2), (Cl^-)•(CH_2Br_2), (Br^-)•(CH_2Cl_2), and (Br^-)•(CH_2Br_2).

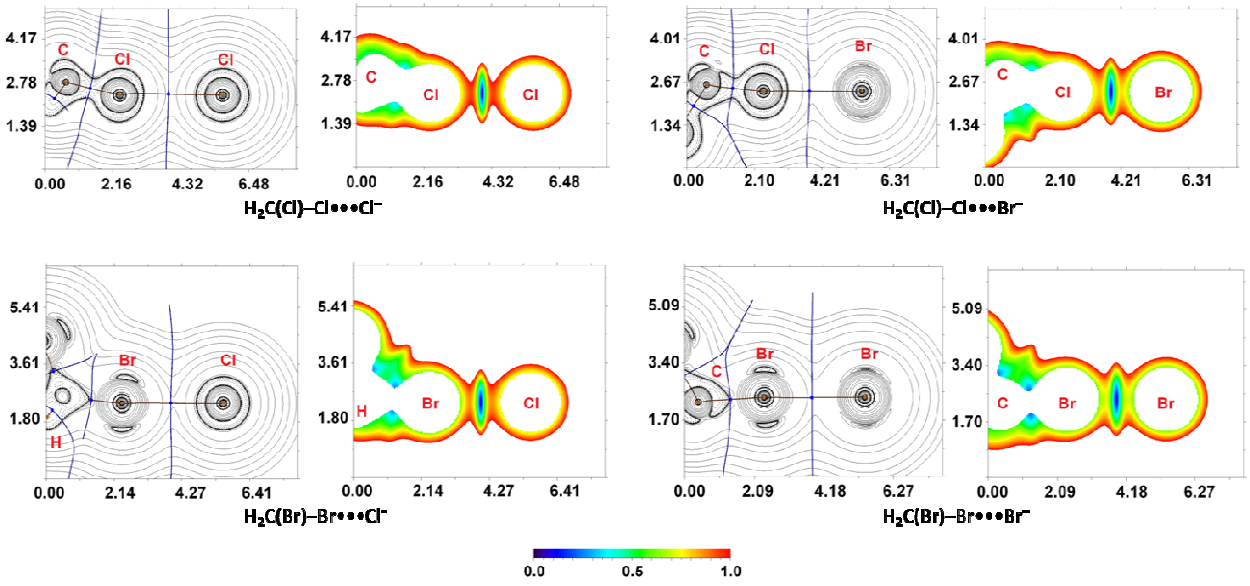

Figure 7. Contour line diagrams of the Laplacian distribution $\nabla^2\rho(\mathbf{r})$, bond paths, and selected zero-flux surfaces (left) and RDG isosurfaces referring to the XBs (right) for the optimized structures of (Cl^-)•(CH_2Cl_2), (Cl^-)•(CH_2Br_2), (Br^-)•(CH_2Cl_2), and (Br^-)•(CH_2Br_2). Bond critical

points (3, –1) are shown in blue, nuclear critical points (3, –3) – in pale brown. Length units – Å, RDG isosurface values are given in Hartree.

We additionally evaluated the magnitude of intermolecular interaction energies in the XBs linked clusters $(Cl^-)\bullet(CH_2Cl_2)$, $(Cl^-)\bullet(CH_2Br_2)$, $(Br^-)\bullet(CH_2Cl_2)$, and $(Br^-)\bullet(CH_2Br_2)$ by supermolecule method using both coupled cluster approach and second order Møller–Plesset perturbation theory at the CCSD(T)/aug-cc-pVDZ//M06/DZP-DKH and MP2/aug-cc-pVDZ//M06/DZP-DKH computational levels. The obtained values of intermolecular interaction energies are higher than those obtained from QTAIM analysis, but lower than calculated vertical dissociation energies at the M06/aug-cc-pVDZ//M06/DZP-DKH level of theory (**Table 5**). The intermolecular interaction energy turns larger with the increase of σ-hole on XB donor and the polarizability decrease of the XB acceptors along the following series $H_2C(Cl)–Cl\bullet\bullet\bullet Br^-$ < $H_2C(Cl)–Cl\bullet\bullet\bullet Cl^-$ < $H_2C(Br)–Br\bullet\bullet\bullet Br^-$ < $H_2C(Br)–Br\bullet\bullet\bullet Cl^-$.

Table 5. The calculated vertical dissociation energies ΔE_1 (CCSD(T)/aug-cc-pVDZ//M06/DZP-DKH), ΔE_2 (MP2/aug-cc-pVDZ//M06/DZP-DKH), and ΔE_3 (M06/aug-cc-pVDZ//M06/DZP-DKH) of XBs linked optimized clusters $(Cl^-)\bullet(CH_2Cl_2)$, $(Cl^-)\bullet(CH_2Br_2)$, $(Br^-)\bullet(CH_2Cl_2)$, and $(Br^-)\bullet(CH_2Br_2)$ (in kcal/mol).

Process	ΔE_1	ΔE_2	ΔE_3
$(Cl^-)\bullet(CH_2Br_2) \rightarrow CH_2Br_2 + Cl^-$	9.5	10.0	12.5
$(Br^-)\bullet(CH_2Br_2) \rightarrow CH_2Br_2 + Br^-$	8.2	8.9	11.0
$(Cl^-)\bullet(CH_2Cl_2) \rightarrow CH_2Cl_2 + Cl^-$	3.9	4.2	5.6
$(Br^-)\bullet(CH_2Cl_2) \rightarrow CH_2Cl_2 + Br^-$	3.0	3.4	4.4

We have defined energies for all these contacts according to the procedures proposed by Espinosa et al.[56] and Vener et al.,[57] and one can state that: (*i*) strengths of XBs in these systems varies from 1.9 to 2.8 kcal/mol; (*ii*) the energies of C–X•••Cl^- XBs for X = Br in all cases are higher than those for X = Cl by 13–47%. This observation agrees well with the previously reported[17] and calculated (**Table 1**) electrostatic potentials on the halogen atoms in CH_2Br_2 and CH_2Cl_2; (*iii*) the strongest N–H•••Cl^- HB's may be classified as moderate force contacts (> 4 kcal/mol) mainly due to electrostatics following the classification of Jeffrey (''strong'' H-bonds: 40–15 kcal/mol, ''moderate'' H-bonds: 15–4 kcal/mol, ''weak'' H-bonds: <4 kcal/mol).[68] Thus, results of our theoretical calculations confirm the presence and provide the energies of the previously unreported $H_2C(X)$–X•••X^- (X = Cl, Br) XBs involving uncomplexed halides. Results of our calculations can be compared with the data obtained at the MP2/aug-cc-pVDZ level of theory for XBs in TEMPO•CH_2Cl_2 (2.5 kcal/mol) and TEMPO•CH_2Br_2 (3.7 kcal/mol) supramolecular clusters.[17] The larger evaluated energies of XBs in cases of anions as XB acceptors (3.4 and 4.2 kcal/mol for CH_2Cl_2 as XB donor; 8.9 and 10.0 kcal/mol for CH_2Br_2 as XB donor) can be explained by charge reasons.

Verification of $H_2C(X)$–X•••X^- (X = Cl, Br) XBs in other systems. We processed available CCDC data and found nine structures exhibiting $H_2C(Cl)$–Cl•••Cl^- XBs (**Table 6**) and four structures with $H_2C(Cl)$–Cl•••Br^- XBs (**Table 7**) accordingly to their geometric parameters; all these contacts were overlooked in the corresponding reports. The $H_2C(Br)$–Br•••X^- XBs were not found although the $H_2C(Br)$–Br•••Cl–Pt XBs with metal-bound chloride were previously reported by us[36] and the $H_2C(Br)$–Br•••Br–C XBs were observed in the crystalline dibromomethane.[69,70] Remarkable that XB in **3a**•CH_2Cl_2 is the shortest chlorine•••chlorine separation involving dihalomethane so far recognized.

Table 6. The parameters of the $H_2C(Cl)–Cl•••Cl^-$ XBs obtained from CCDC data processing.

Structure	*d*(Cl•••Cl), Å	R_{ClCl}	∠(C–Cl•••Cl),°
EZAPIE	3.3466(18)	0.95	166.84(11)
LOBGIT	3.371(6)	0.96	163.5(6)
PACVOG	3.5097(10)	1.00	174.99(12)
QACNEP	3.265(2)	0.93	173.31(14)
	3.3616(19)	0.96	167.0(2)
	3.3841(19)	0.96	170.8(2)
SUNMUL	3.4545(16)	0.98	177.32(3)
WUYSEP	3.496(2)	0.99	166.23(18)
XERTOE	3.4189(8)	0.97	161.94(9)
YEDPEC	3.4932(16)	0.99	160.33(10)
ZETBOR	3.443(2)	0.98	169.7(2)
This work	3.276(3)	0.93	166.3(3)
	3.236(2)	0.92	166.2(4)
Comparison[a]	*3.52 (Cl•••Cl)*	*1.00*	*180*

[a]*Comparison is the sum of Rowland's vdW radii and the classic XB angle.*

Table 7. The parameters of the $H_2C(Cl)–Cl•••Br^-$ XBs obtained from CCDC data processing.

Structure	*d*(Cl•••Br), Å	R_{ClBr}	∠(C–Cl•••Br),°
AJUZUA	3.5493(15)	0.98	172.0(2)
BOHTIG	3.3972(18)	0.94	170.0(3)

IHUGUO	3.5284(17)	0.97	169.5(3)
MOWBEG	3.101(8)	0.85	173.8(9)
Comparison[a]	*3.63 (Cl•••Cl)*	*1.00*	*180*

[a] *Comparison is the sum of Rowland's vdW radii and the classic XB angle.*

Concluding Remarks

A series of the *cis*-[PdX(CNCy){C(NHCy)=NHC$_6$H$_2$Me$_2$NH$_2$}]X•CH$_2$X$_2$ (X = Cl, Br) associates with the dihalomethanes were characterized by XRD. In the structures of **3a**•CH$_2$Cl$_2$, **3a**•CH$_2$Br$_2$, and **4**•CH$_2$Br$_2$, we detected the previously unreported H$_2$C(X)–X•••X$^-$ (X = Cl, Br) contacts with uncomplexed halides that fulfill the IUPAC criteria for the halogen bonding. Results of Bader's QTAIM analysis (M06/DZP-DKH level of theory) reveal that estimated strength of these XBs varies from 1.9 to 2.8 kcal/mol and that these contacts are actually non-covalent; the crystal packing significantly affects the lengths and energies of XBs.

Our processing of the available CCDC data allowed the recognition of some more H$_2$C(Cl)–Cl•••X$^-$ (X = Cl, Br) halogen bonds, but no H$_2$C(Br)–Br•••X$^-$ (X = Cl, Br) XBs were found. All contacts presented in **Tables 6** and **7** were overlooked in the corresponding papers. It is clear that the XB in **3a**•CH$_2$Cl$_2$ is the shortest chlorine•••chlorine separation involving dihalomethane so far recognized.

The results reported in this work can be used as starting point for further studies of XBs in dihalomethane solutions, where they may be sufficiently strong to contribute, along with H-bonding, to the overall solvation. We hope that our observation will be beneficial for both crystal

engineering and physical chemistry communities because it expands the arsenal of supramolecular assembly and contributes to the understanding of solvation with dihalomethanes.

Experimental section

Materials and Instrumentation. Solvents, $PdCl_2$, and cyclohexyl isocyanide were obtained from commercial sources and used as received, whereas CH_2Cl_2 was purified by the conventional distillation over calcium chloride. 3,4-Dimethylbenzene-1,2-diamine was synthesized from 3,4-dimethylaniline (synthetic procedure can be found in Supporting Information).[71] Complex **3a** was synthesized by the reported procedure[48] and **4** was synthesized from **3a** by metathesis with KBr in acetone.[72] C, H, and N elemental analyses were carried out on a Euro EA 3028HT CHNS/O analyzer. Mass-spectra were obtained on a Bruker micrOTOF spectrometer equipped with electrospray ionization (ESI) source; MeOH was used as the solvent. The instrument was operated both at positive and negative ion modes using *m/z* range of 50–3000. The capillary voltage of the ion source was set at –4500 V (ESI^+) or 3500 V (ESI^-) and the capillary exit at ±(70–150) V. The nebulizer gas pressure was 0.4 bar and drying gas flow 4.0 L/min. The NMR spectra were recorded on Bruker AVANCE III 400 spectrometer at ambient temperature in $CDCl_3$ (at 400, and 100 MHz for ^1H and $^{13}C\{^1H\}$ NMR spectra, respectively). Chemical shifts are given in δ-values [ppm] referenced to the residual signals of non-deuterated solvent ($CHCl_3$): δ 7.26 (^1H) and 77.2 (^{13}C). ^1H and $^{13}C\{^1H\}$ NMR data assignment for **4** produced by using 2D (^1H,^{13}C-HMQC/HSQC and ^1H,^{13}C-HMBC) NMR correlation experiments.

Synthesis, crystallization, and structure refinement. *Synthesis of* **4**. Solid KBr (480 mg, 4 mmol) was added to a suspension of **3a** (53 mg, 0.1 mmol) in acetone (4 mL) at 20–25 ºC

and the reaction mixture was stirred at RT for 1 d. The formed suspension was evaporated at 40–45 ºC under normal pressure and the product was extracted with three 2-mL portions of CH_2Cl_2. The resulting bright yellow solution was filtered off to remove some insoluble material, the filtrate was evaporated at RT to dryness, and thus formed solid was dried in air at 20–25 °C.

4•CH_2Cl_2. Yield 93%. Calc. for $C_{23}H_{36}N_4Br_2Cl_2Pd$: C, 39.15; H, 5.14; N, 7.94. Found: C, 39.30; H, 5.17; N, 7.99. HRESI$^+$-MS (70 V, MeOH): calc. for $C_{22}H_{34}N_4BrPd^+$ 539.0996, found *m/z* 539.1004 $[M - Br]^+$. IR (KBr, selected bands, cm^{-1}): ν(N–H) 3180 (m), ν(C–H) 2930–2854 (m), ν(C≡N) 2234 (s), ν(N–$C_{carbene}$) 1570 (s), δ(N–H) 1514 (s). ^{1}H NMR ($CDCl_3$, δ): 0.86–1.91 (20H, m, CH_2), 2.08 (3H, s, CH_3), 2.18 (3H, s, CH_3), 3.67–3.70 (1H, m, CH), 3.83–3.86 (1H, m, CH), 5.30 (2H, s, CH_2Cl_2), 6.71 (1H, s, H_{Ar}), 6.91 (1H, s, H_{Ar}), 9.24–9.27 (1H, m, $C_{carbene}$–N*H*–Cy), 10.66 (1H, s, NH). ^{13}C{^{1}H} NMR ($CDCl_3$, δ): 19.03 (CH_3), 19.07 (CH_3), 22.58 ($2CH_2$), 24.47 (CH_2), 24.71 ($3CH_2$), 31.77 ($2CH_2$), 33.88 ($2CH_2$), 53.39 (CH_2Cl_2), 55.68 (CH), 59.17 (CH), 122.15(CH_{Ar}), 122.77 (CH_{Ar}), 123.61 (C≡N), 124.55(C_{Ar}), 133.03 (C_{Ar}), 133.69 (C_{Ar}), 135.38 (C_{Ar}), 179.06 ($C_{carbene}$).

Crystals of **3a**•CH_2Cl_2, **3a**•CH_2Br_2, **4**•CH_2Cl_2, and **4**•CH_2Br_2 were obtained upon slow evaporation of a solution of **3a** or **4**•CH_2Cl_2 in CH_2Cl_2 and CH_2Br_2, respectively, in air at RT. Details of structure solutions and refinements can be found in SI.

Computational Details. Unless otherwise indicated, the single point calculations and full geometry optimization have been carried out at the DFT level of theory using the M06 functional[73] (this functional describes reasonably weak dispersion forces and non-covalent interactions[74,75]) with the help of Gaussian-09[76] program package. The Douglas–Kroll–Hess 2nd order scalar relativistic calculations requested relativistic core Hamiltonian were carried out

using DZP-DKH basis sets[77-83] for all atoms based on the experimentally obtained X-ray geometries ((*cis*-[PdCl(CNCy){C(NHCy)=NHC$_6$H$_2$Me$_2$NH$_2$}]$^+$)$_6$•(Cl$^-$)$_2$•(CH$_2$Cl$_2$)$_2$ (two types), (*cis*-[PdCl(CNCy){C(NHCy)=NHC$_6$H$_2$Me$_2$NH$_2$}]$^+$)$_6$•(Cl$^-$)$_2$•(CH$_2$Br$_2$)$_2$, (Cl$^-$)•(CH$_2$Cl$_2$) (two types), and (Cl$^-$)•(CH$_2$Br$_2$)) or optimized equilibrium structures ((Cl$^-$)•(CH$_2$Cl$_2$) (two types) and (Cl$^-$)•(CH$_2$Br$_2$)). No symmetry restrictions have been applied during the geometry optimization. The Hessian matrix was calculated analytically for optimized structures to prove the location of correct minima (no imaginary frequencies). The topological analysis of the electron density distribution with the help of the atoms in molecules (QTAIM) method developed by Bader[84] has been performed by using the Multiwfn program (version 3.3.4).[85]

ASSOCIATED CONTENT

Supporting Information.

The following files are available free of charge:

additional data from the literature: maximum σ-hole potentials of halomethane molecules and geometrical parameters of the halomethane–halide XBs; full crystal data description; full HB description; NMR and IR spectra; additional results of the theoretical calculations; and synthesis of 1,2-diamino-4,5-dimethylbenzene from 3,4-dimethylaniline; all in one PDF file.

AUTHOR INFORMATION

Corresponding Author

*Vadim Yu. Kukushkin

e-mail: v.kukushkin@spbu.ru

Funding Sources

ACKNOWLEDGMENT

The authors thank the Russian Foundation for Basic Research (grants 16-33-60063 and 16-33-60123), the Grant Program of the President of Russian Federation (Grant MK-7425.2016.3), and RAS Program 1.14P for financial support. IVA gratefully acknowledges the Russian Foundation for Basic Research (grant 16-33-60133) for financial support of the X-ray diffraction studies. Physicochemical studies were performed at the Center for Magnetic Resonance, Center for X-ray Diffraction Studies, Center for Chemical Analysis and Materials Research (all belong to Saint Petersburg State University).

ABBREVIATIONS

HB, hydrogen bonding; XB, halogen bonding; XRD, X-ray diffraction; NMR, nuclear magnetic resonance; EPR, electron paramagnetic resonance; IR, infrared; TLC, thin layer chromatography; TEMPO, 2,2,6,6-tetramethyl-1-piperidin-1-yloxy free radical; ESP, electrostatic surface potential; RDG, reduced density gradient; QTAIM, quantum theory of atoms in molecules.

REFERENCES

(1) Busschaert, N.; Caltagirone, C.; Van Rossom, W.; Gale, P. A. *Chem. Rev.* **2015**, *115*, 8038–8155.

(2) Agmon, N.; Bakker, H. J.; Campen, R. K.; Henchman, R. H.; Pohl, P.; Roke, S.; Thämer, M.; Hassanali, A. *Chem. Rev.* **2016**, *116*, 7642–7672.

(3) van der Vegt, N. F. A.; Haldrup, K.; Roke, S.; Zheng, J.; Lund, M.; Bakker, H. J. *Chem. Rev.* **2016**, *116*, 7626–7641.

(4) Tielrooij, K. J.; Garcia-Araez, N.; Bonn, M.; Bakker, H. J. *Science* **2010**, *328*, 1006–1009.

(5) Tobias, D. J.; Hemminger, J. C. *Science* **2008**, *319*, 1197–1198.

(6) Fournier, J. A.; Carpenter, W.; De Marco, L.; Tokmakoff, A. *J. Am. Chem. Soc.* **2016**, doi: 10.1021/jacs.6b05122.

(7) DiTucci, M. J.; Heiles, S.; Williams, E. R. *J. Am. Chem. Soc.* **2015**, *137*, 1650–1657.

(8) Ford, D. D.; Lehnherr, D.; Kennedy, C. R.; Jacobsen, E. N. *ACS Catal.* **2016**, *6*, 4616–4620.

(9) Mittal, N.; Lippert, K. M.; De, C. K.; Klauber, E. G.; Emge, T. J.; Schreiner, P. R.; Seidel, D. *J. Am. Chem. Soc.* **2015**, *137*, 5748–5758.

(10) Lehnherr, D.; Ford, D. D.; Bendelsmith, A. J.; Kennedy, C. R.; Jacobsen, E. N. *Org. Lett.* **2016**, *18*, 3214–3217.

(11) Langton, M. J.; Serpell, C. J.; Beer, P. D. *Angew. Chem., Int. Ed.* **2016**, *55*, 1974–1987.

(12) Evans, N. H.; Beer, P. D. *Angew. Chem., Int. Ed.* **2014**, *53*, 11716–11754.

(13) Saha, T.; Hossain, M. S.; Saha, D.; Lahiri, M.; Talukdar, P. *J. Am. Chem. Soc.* **2016**, *138*, 7558–7567.

(14) Berryman, O. B.; Sather, A. C.; Hay, B. P.; Meisner, J. S.; Johnson, D. W. *J. Am. Chem. Soc.* **2008**, *130*, 10895–10897.

(15) Cai, J.; Sessler, J. L. *Chem. Soc. Rev.* **2014**, *43*, 6198–6213.

(16) Clark, T.; Hennemann, M.; Murray, J. S.; Politzer, P. *J. Mol. Model.* **2007**, *13*, 291–296.

(17) Pang, X.; Jin, W. J. *New J. Chem.* **2015**, *39*, 5477–5483.

(18) Bundhun, A.; Ramasami, P.; Murray, J. S.; Politzer, P. *J. Mol. Model.* **2013**, *19*, 2739–2746.

(19) Rosokha, S. V.; Stern, C. L.; Ritzert, J. T. *Chem.-Eur. J.* **2013**, *19*, 8774–8788.

(20) Rosokha, S. V.; Neretin, I. S.; Rosokha, T. Y.; Hecht, J.; Kochi, J. K. *Heteroatom Chem.* **2006**, *17*, 449–459.

(21) Lindeman, S. V.; Hecht, J.; Kochi, J. K. *J. Am. Chem. Soc.* **2003**, *125*, 11597–11606.

(22) Bock, H.; Holl, S. *Z.Naturforsch.(B)* **2001**, *56*, 152–163.

(23) Lohr, H. G.; Engel, A.; Josel, H. P.; Vogtle, F.; Schuh, W.; Puff, H. *Journal of Organic Chemistry* **1984**, *49*, 1621–1627.

(24) Kodiah Beyeh, N.; Cetina, M.; Rissanen, K. *Chem. Commun.* **2014**, *50*, 1959–1961.

(25) Cavallo, G.; Biella, S.; Lu, J. A.; Metrangolo, P.; Pilati, T.; Resnati, G.; Terraneo, G. *J. Fluor. Chem.* **2010**, *131*, 1165–1172.

(26) Gushchin, P. V.; Starova, G. L.; Haukka, M.; Kuznetsov, M. L.; Eremenko, I. L.; Kukushkin, V. Y. *Cryst. Growth Des.* **2010**, *10*, 4839–4846.

(27) Allen, F. H.; Wood, P. A.; Galek, P. T. A. *Acta Crystallogr. Sect. B-Struct. Sci.* **2013**, *69*, 379–388.

(28) Mooibroek, T. J.; Gamez, P. *CrystEngComm* **2013**, *15*, 4565–4570.

(29) Bertrán, J. F.; Rodríguez, M. *Org. Magn. Reson.* **1980**, *14*, 244–246.

(30) Podsiadło, M.; Dziubek, K.; Szafranski, M.; Katrusiak, A. *Acta Crystallogr. Sect. B-Struct. Sci.* **2006**, *62*, 1090–1098.

(31) Podsiadło, M.; Katrusiak, A. *CrystEngComm* **2008**, *10*, 1436–1442.

(32) Sureshan, K. M.; Gonnade, R. G.; Shashidhar, M. S.; Puranik, V. G.; Bhadbhade, M. M. *Chem. Commun.* **2001**, 881–882.

(33) Alshahateet, S. F.; Bishop, R.; Craig, D. C.; Scudder, M. L. *Cryst. Growth Des.* **2011**, *11*, 4474–4483.

(34) Podsiadło, M.; Dziubek, K.; Katrusiak, A. *Acta Crystallogr. Sect. B-Struct. Sci.* **2005**, *61*, 595–600.

(35) Brammer, L.; Espallargas, G. M.; Libri, S. *CrystEngComm* **2008**, *10*, 1712–1727.

(36) Ivanov, D. M.; Novikov, A. S.; Starova, G. L.; Haukka, M.; Kukushkin, V. Y. *CrystEngComm* **2016**, *18*, 5278–5286.

(37) Gushchin, P. V.; Kuznetsov, M. L.; Wang, Q.; Karasik, A. A.; Haukka, M.; Starova, G. L.; Kukushkin, V. Y. *Dalton Trans.* **2012**, *41*, 6922–6931.

(38) Gushchin, P. V.; Kuznetsov, M. L.; Haukka, M.; Kukushkin, V. Y. *J. Phys. Chem. A* **2014**, *118*, 9529−9539.

(39) Kopylovich, M. N.; Tronova, E. A.; Haukka, M.; Kirillov, A. M.; Kukushkin, V. Y.; Frafisto da Silva, J. J. R.; Pombeiro, A. J. L. *Eur. J. Inorg. Chem.* **2007**, 4621–4627.

(40) Serebryanskaya, T. V.; Novikov, A. S.; Gushchin, P. V.; Haukka, M.; Asfin, R. E.; Tolstoy, P. M.; Kukushkin, V. Y. *Phys. Chem. Chem. Phys.* **2016**, *18*, 14104–14112.

(41) Luzyanin, K. V.; Tskhovrebov, A. G.; Carias, M. C.; Guedes da Silva, M. F. C.; Pombeiro, A. J. L.; Kukushkin, V. Y. *Organometallics* **2009**, *28*, 6559–6566.

(42) Valishina, E. A.; da Silva, M.; Kinzhalov, M. A.; Timofeeva, S. A.; Buslaeva, T. M.; Haukka, M.; Pombeiro, A. J. L.; Boyarskiy, V. P.; Kukushkin, V. Y.; Luzyanin, K. V. *J. Mol. Catal. A-Chem.* **2014**, *395*, 162–171.

(43) Boyarskiy, V. P.; Luzyanin, K. V.; Kukushkin, V. Y. *Coord. Chem. Rev.* **2012**, *256*, 2029–2056.

(44) Kinzhalov, M. A.; Luzyanin, K. V.; Boyarskiy, V. P.; Haukka, M.; Kukushkin, V. Y. *Organometallics* **2013**, *32*, 5212–5223.

(45) Kinzhalov, M. A.; Boyarskii, V. P. *Russ. J. Gen. Chem.* **2015**, *85*, 2313–2333.

(46) Timofeeva, S. A.; Kinzhalov, M. A.; Valishina, E. A.; Luzyanin, K. V.; Boyarskiy, V. P.; Buslaeva, T. M.; Haukka, M.; Kukushkin, V. Y. *J. Catal.* **2015**, *329*, 449–456.

(47) Rocha, B. G. M.; Valishina, E. A.; Chay, R. S.; da Silva, M.; Buslaeva, T. M.; Pombeiro, A. J. L.; Kukushkin, V. Y.; Luzyanin, K. V. *J. Catal.* **2014**, *309*, 79–86.

(48) Kinzhalov, M. A.; Timofeeva, S. A.; Luzyanin, K. V.; Boyarskiy, V. P.; Yakimanskiy, A. A.; Haukka, M.; Kukushkin, V. Y. *Organometallics* **2016**, *35*, 218–228.

(49) Kinzhalov, M. A.; Starova, G. L.; Boyarskiy, V. P. *Inorganica Chimica Acta* **2016**, *455, Part 2*, 607–612.

(50) Kinzhalov, M. A.; Novikov, A. S.; Chernyshev, A. N.; Suslonov, V. V. *Z. Krist. – Cryst. Mater.* **2016**, accepted.

(51) Desiraju, G. R.; Ho, P. S.; Kloo, L.; Legon, A. C.; Marquardt, R.; Metrangolo, P.; Politzer, P.; Resnati, G.; Rissanen, K. *Pure Appl. Chem.* **2013**, *85*, 1711–1713.

(52) Rowland, R. S.; Taylor, R. *J. Phys. Chem.* **1996**, *100*, 7384–7391.

(53) Mukherjee, A.; Tothadi, S.; Desiraju, G. R. *Accounts Chem. Res.* **2014**, *47*, 2514–2524.

(54) Johnson, M. T.; Dzolic, Z.; Cetina, M.; Wendt, O. F.; Ohrstrom, L.; Rissanen, K. *Cryst. Growth Des.* **2012**, *12*, 362–368.

(55) Yufit, D. S.; Shishkin, O. V.; Zubatyuk, R. I.; Howard, J. A. K. *Cryst. Growth Des.* **2014**, *14*, 4303–4309.

(56) Espinosa, E.; Molins, E.; Lecomte, C. *Chem. Phys. Lett.* **1998**, *285*, 170–173.

(57) Vener, M. V.; Egorova, A. N.; Churakov, A. V.; Tsirelson, V. G. *J. Comput. Chem.* **2012**, *33*, 2303–2309.

(58) Bader, R. F. W. *Chem. Rev.* **1991**, *91*, 893–928.

(59) Novikov, A. S.; Kuznetsov, M. L.; Pombeiro, A. J. L. *Chem.-Eur. J.* **2013**, *19*, 2874–2888.

(60) Ivanov, D. M.; Novikov, A. S.; Ananyev, I. V.; Kirina, Y. V.; Kukushkin, V. Y. *Chem. Comm.* **2016**, *52*, 5565−5568.

(61) Ding, X.; Tuikka, M. J.; Hirva, P.; Kukushkin, V. Y.; Novikov, A. S.; Haukka, M. *CrystEngComm* **2016**, *18*, 1987–1995.

(62) Mikhaylov, V. N.; Sorokoumov, V. N.; Korvinson, K. A.; Novikov, A. S.; Balova, I. A. *Organometallics* **2016**, *35*, 1684–1697.

(63) Mikherdov, A. S.; Kinzhalov, M. A.; Novikov, A. S.; Boyarskiy, V. P.; Boyarskaya, I. A.; Dar'in, D. V.; Starova, G. L.; Kukushkin, V. Y. *J. Am. Chem. Soc.* **2016**, *138*, 14129–14137.

(64) Yandanova, E. S.; Ivanov, D. M.; Kuznetsov, M. L.; Starikov, A. G.; Starova, G. L.; Kukushkin, V. Y. *Cryst. Growth Des.* **2016**, *16*, 2979−2987.

(65) Andrusenko, E.; Kabin, E.; Novikov, A. S.; Bokach, N. A.; Starova, G. L.; Kukushkin, V. Y. *New Journal of Chemistry* **2016**, Accepted manuscript, doi: 10.1039/c6nj02962k.

(66) Espinosa, E.; Alkorta, I.; Elguero, J.; Molins, E. *J. Chem. Phys.* **2002**, *117*, 5529–5542.

(67) Johnson, E. R.; Keinan, S.; Mori-Sánchez, P.; Contreras-García, J.; Cohen, A. J.; Yang, W. *Journal of the American Chemical Society* **2010**, *132*, 6498–6506.

(68) Steiner, T. *Angew. Chem.-Int. Edit.* **2002**, *41*, 48–76.

(69) Kawaguchi, T.; Wakabayashi, A.; Matsumoto, M.; Takeuchi, T.; Watanabe, T. *Bull. Chem. Soc. J.* **1973**, *46*, 57–61.

(70) Podsiadlo, M.; Dziubek, K.; Szafranski, M.; Katrusiak, A. *Acta Crystallogr. Sect. B-Struct. Sci.* **2006**, *62*, 1090–1098.

(71) Chattopadhyay, P.; Nagpal, R.; Pandey, P. S. *Australian Journal of Chemistry* **2008**, *61*, 216–222.

(72) Kinzhalov, M. A.; Luzyanin, K. V.; Boyarskaya, I. A.; Starova, G. L.; Boyarskiy, V. P. *J. Mol. Struct.* **2014**, *1068*, 222–227.

(73) Zhao, Y.; Truhlar, D. G. *Theoretical Chemistry Accounts* **2008**, *120*, 215–241.

(74) Kozuch, S.; Martin, J. M. L. *J. Chem. Theory Comput.* **2013**, *9*, 1918−1931.

(75) Bauzá, A.; Alkorta, I.; Frontera, A.; Elguero, J. *J. Chem. Theory Comput.* **2013**, *9*, 5201−5210.

(76) Frisch, M. J.; Trucks, G. W.; Schlegel, H. B.; Scuseria, G. E.; Robb, M. A.; Cheeseman, J. R.; Scalmani, G.; Barone, V.; Mennucci, B.; Petersson, G. A.; Nakatsuji, H.; Caricato, M.; Li, X.; Hratchian, H. P.; Izmaylov, A. F.; Bloino, J.; Zheng, G.; Sonnenberg, J. L.; Hada, M.; Ehara, M.; Toyota, K.; Fukuda, R.; Hasegawa, J.; Ishida, M.; Nakajima, T.; Honda, Y.; Kitao, O.; Nakai, H.; Vreven, T.; A.;, M. J.; Peralta, J. E.; Ogliaro, F.; Bearpark, M.; Heyd, J. J.; Brothers, E.; Kudin, K. N.; Staroverov, V. N.; Keith, T.; Kobayashi, R.; Normand, J.; Raghavachari, K.; Rendell, A.; Burant, J. C.; Iyengar, S. S.; Tomasi, J.; Cossi, M.; Rega, N.; Millam, J. M.; Klene, M.; Knox, J. E.; Cross, J. B.; Bakken, V.; Adamo, C.; Jaramillo, J.; Gomperts, R.; Stratmann, R. E.; Yazyev, O.; Austin, A. J.; Cammi, R.; Pomelli, C.; Ochterski, J. W.; Martin, R. L.; Morokuma, K.; Zakrzewski, V. G.; Voth, G. A.; Salvador, P.; Dannenberg, J. J.; Dapprich, S.; Daniels, A. D.; Farkas, O.; Foresman, J. B.; Ortiz, J. V.; J.;, C.; Fox, D. J. In *Gaussian 09, Revision C.01*; Gaussian, Inc.: Wallingford, CT, 2010.

(77) Barros, C. L.; de Oliveira, P. J. P.; Jorge, F. E.; Neto, A. C.; Campos, M. *Mol. Phys.* **2010**, *108*, 1965–1972.

(78) Jorge, F. E.; Neto, A. C.; Camiletti, G. G.; Machado, S. F. *Journal of Chemical Physics* **2009**, *130*, 6.

(79) Neto, A. C.; Jorge, F. E. *Chem. Phys. Lett.* **2013**, *582*, 158–162.

(80) de Berredo, R. C.; Jorge, F. E. *Journal of Molecular Structure - Theochem* **2010**, *961*, 107–112.

(81) Barros, C. L.; de Oliveira, P. J. P.; Jorge, F. E.; Neto, A. C.; Campos, M. *Molecular Physics* **2010**, *108*, 1965–1972.

(82) Jorge, F. E.; Neto, A. C.; Camiletti, G. G.; Machado, S. F. *Journal of Chemical Physics* **2009**, *130*, 064108.

(83) Neto, A. C.; Jorge, F. E. *Chemical Physics Letters* **2013**, *582*, 158–162.

(84) Bader, R. F. W. *Atoms in Molecules: A Quantum Theory, Oxford University Press, Oxford* **1990**.

(85) Lu, T.; Chen, F. W. *Journal of Computational Chemistry* **2012**, *33*, 580–592.

For Table of Contents Use Only

The $H_2C(X)–X•••X^-$ (X = Cl, Br) Halogen Bonding of Dihalomethanes

Daniil M. Ivanov, Mikhail A. Kinzhalov, Alexander S. Novikov, Ivan V. Ananyev, Anna A. Romanova, Vadim P. Boyarskiy, Matti Haukka, and Vadim Yu. Kukushkin

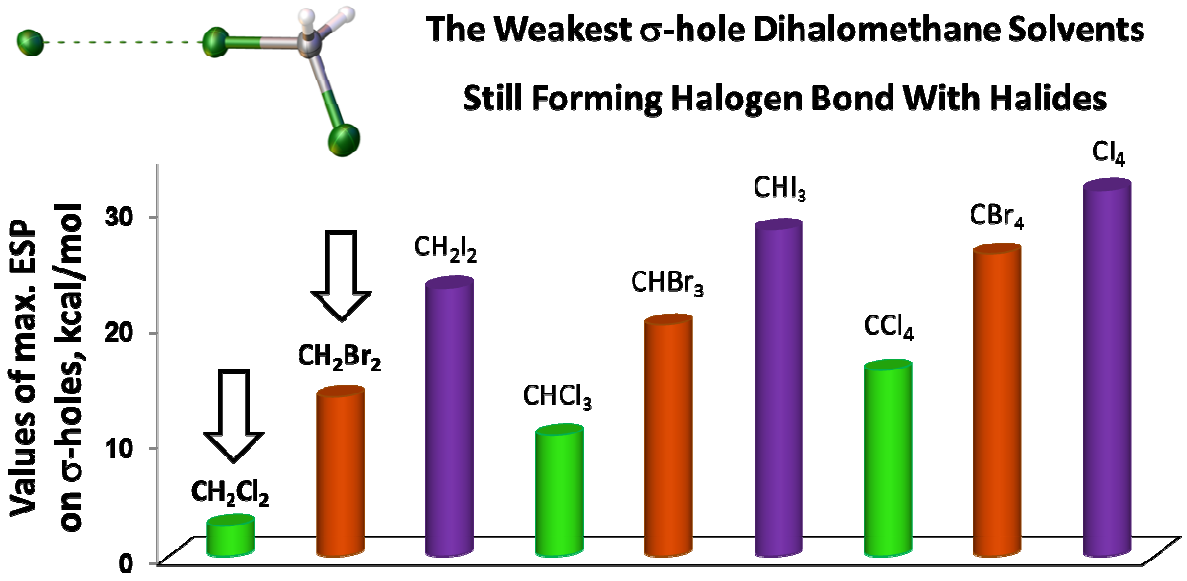

SYNOPSIS

The weakest σ-hole dichloromethane and dibromomethane still form XBs with chloride in bromide in the solvates of acyclic diaminocarbene palladium(II) complex used as a scaffold. The estimated bonding energies of the $H_2C(X)–X•••X^-$ non-covalent interactions is in the 1.9–2.8 kcal/mol range.